Hindawi
Adsorption Science & Technology
Volume 2022, Article ID 4249949, 11 pages
https://doi.org/10.1155/2022/4249949

Research Article

Influence of the Branched Structure of Polyoxyethylene Units in Nonionic Surfactants on the Wettability of Anthracite: A Combined Modeling and Experimental Study

Xuanlai Chen[1], **Guochao Yan**[1], **Guang Xu**[2], **Xianglin Yang**[3], **Jiajun Li**[1], **and Xuyang Bai**[1]

[1]*School of Mining Engineering, Taiyuan University of Technology, Taiyuan 030024, China*
[2]*Department of Mining Engineering, Missouri University of Science and Technology, Rolla, MO 65409, USA*
[3]*Hunan Provincial Key Laboratory of Fine Ceramics and Powder Materials, School of Materials and Environmental Engineering, Hunan University of Humanities, Science and Technology, Loudi 417000, China*

Correspondence should be addressed to Guochao Yan; yanguochao@tyut.edu.cn

Received 24 March 2022; Accepted 5 May 2022; Published 21 May 2022

Academic Editor: George Kyzas

Coal dust is a significant concern to the safety of coal mine operations. The wettability of coal can be effectively altered by adding surfactants to water. The development of high-efficiency dust suppressants is hampered by a lack of understanding of the microscopic interaction process between coal dust and surfactants. In this investigation, the influence of the branched structure of the polyoxyethylene unit in nonionic surfactants on the wettability of anthracite surfaces was evaluated by combining the modeling study and experimental research. The macromolecular model of Jincheng anthracite with 55 different components ($C_{7730}H_{3916}O_{133}N_{123}S_{25}$) was constructed. Lauryl polyoxyethylene ether $C_{12}(EO)_{20}$ and Tween 20 were selected. The simulation results showed that due to the branched structure of polyoxyethylene, the surface of anthracite after adsorption by Tween 20 is more hydrophilic. Further analysis found that the adsorption configuration of Tween 20 is that the hydrophilic head group covers the hydrophobic tail chain, while the adsorption configuration of $C_{12}(EO)_{20}$ is that the hydrophobic tail chain covers the hydrophilic head group. The network structure formed by Tween 20 is relatively loose, and the surface is rougher. The network structure formed by $C_{12}(EO)_{20}$ is denser. Water molecules have a higher aggregation degree near Tween 20 and stronger permeability, and more hydrogen bonds are formed. The existence state of carbon and oxygen elements on the surface of modified coal was analyzed by XPS experiment, which confirmed the adsorption structure obtained by molecular simulation.

1. Introduction

Mine dust is made up of minute particles such as rocks and coal that are produced during the development, excavation, mining, and transportation of coal mines. Coal dust is a major source of pollution in coal mines. Coal dust suspends materials exists in the air or as road deposits, which not only reduces worker visibility but also pollutes the working environmentCoal mine dust exists in the air or deposits on roads, which not only reduces the visibility, but also pollutes the surrounding environment. Coal seam spraying is currently widely used to reduce coal dust, which is crucial to coal mine output and safety [1, 2]. Nevertheless, the efficacy of employing water alone for dust reduction is far from ideal due to the abundance of oxygen-containing functional groups on the surface of coal dust [3, 4].

Surfactants have both hydrophobic and hydrophilic groups in their structure, allowing them to effectively alter

coal surface characteristics. The wettability of coal dust can be dramatically altered by adding modest amounts of surfactant to water. Xu et al. [3] found that surfactants changed the wettability of coal by affecting the hydrophobicity and hydrophilicity of the coal surface. Mishra and Panda [5] found that the coal surface became more hydrophobic after being adsorbed by the surfactant. Liu et al. [6] revealed that different surfactants had differentiated hydrophilization ability toward the coal surface.

In recent years, researchers around the world have carried out a large number of experimental studies on surfactants changing coal wettability [4, 7–10]. Empirical investigations, on the other hand, generat primarily macroscopic results, with little discussion of the structure, kinetics, and energy properties of the molecular adsorption process on mineral surfaces. Researchers are increasingly turning to molecular dynamics simulation to investigate changes in coal wettability from a microscopic perspective [11–14]. Notwithstanding, most coal models chosen for the exploration are single-part coal models in the momentum research on the properties of coal interacting with atomic elements [7, 11–25]. The atomic load of this sort of coal model is little, despite the fact that it can portray the attributes of coal partially, it is a long way from the genuine circumstance. In our previous study [26, 27], the two-component Jincheng anthracite model was constructed [28]. The molecular formula of the coal model composed of 40 anthracite molecules is $C_{2360}H_{1440}O_{40}N_{40}$, which is rich in model components. Nonetheless, since the presence of sulfur iotas is not thought of and the atomic load of the model is little, this model can portray the point of interaction properties of anthracite somewhat. Coal is a complex multipart macromolecular natural matter, so the single-part and little atomic weight coal model utilized in the ebb and flow research is still a long way from the genuine circumstance. In this case, a large-molecular weight Jincheng anthracite model ($C_{7730}H_{3916}O_{133}N_{123}S_{25}$) composed of 55 different components through a large number of experiments in the early stage was proposed [29]. This model is utilized to concentrate on the connection point qualities, which is nearer to the genuine circumstance as far as the wealth of the coal model parts and the subatomic weight. The macromolecular coal model requires additional processing assets and longer figuring time, which is a significant hindrance of picking this coal model. The ebb and flow research on coal interface attributes is centered around low-rank coal, while there is little exploration on the point of interaction qualities of high-rank coal. It is a new investigation of the interfacial properties of coal utilizing a multicomponent, high-atomic weight coal model that is nearer to the genuine circumstance. This study will assist individuals with understanding the adsorption interaction and minute component of surfactants on the outer layer of anthracite.

In this investigation, the Jincheng anthracite model ($C_{7730}H_{3916}O_{133}N_{123}S_{25}$) with 55 components and large molecular weight will be selected [29]. The effects of two surfactants, Tween 20 and $C_{12}(EO)_{20}$, with different structures of polyoxyethylene units, on the wettability of anthracite will be studied by experiments and molecular dynamics (MD) simulations. Tween 20 has a similar molecular composition to $C_{12}EO_{20}$, such as 20 total polyoxyethylene units and one equivalent alkyl chain. The main difference between these two surfactants is that the polyoxyethylene units in Tween 20 are spread out on different branches, whereas the polyoxyethylene units in $C_{12}EO_{20}$ are linear. First, a molecular dynamics simulation of the surfactant adsorption process on anthracite surface will be carried out. A surfactant-anthracite binary system will be constructed to compare the interaction energy of surfactants and anthracite by analyzing roughness and interaction energy. A water-surfactant-anthracite ternary system will be constructed, by analyzing the interaction energy of modified coal and water molecules, relative concentration distribution, radial distribution function (RDF), and number of hydrogen bonds, the binding capacity of modified coal to water molecules will be compared. Second, the abovementioned simulation results will be verified by experiments. The existence state of carbon and oxygen elements on the surface of modified coal will be analyzed by XPS experiment. The experimental data are in good agreement with the molecular dynamics simulation evaluation.

2. Experiments and Simulations

2.1. Materials. The anthracite from the Zhaozhuang Coal Mine, Jincheng, Shanxi province, China, was selected as the experimental coal sample, and coal samples with a particle size ranging from 200 to 300 mesh (pore diameter 0.074 mm to 0.050 mm) were selected by crushing and screening. In order to further reduce the influence of inorganic minerals in coal, HCl-HF-HCl acid elution of minerals was carried out and washed in excess distilled water until the pH of the filtrate was neutral. The ash content on dry basis after the treatment was 0.3%, indicating that there were basically no ash-forming minerals. The HCl/HF/HCl treatment may physically change the surface microstructure (e.g., specific pore volume), but the chemical properties of the coal surface remain almost unchanged [30]. Ultimate analyses of Jincheng anthracite are shown in Table 1.

The main chemicals used in this work were $C_{12}EO_{20}$ and Tween 20, which were supplied by the Nanjing Ruichuang Chemical Technology Co. Ltd. Figure 1 shows their molecular structure.

2.2. Molecular Dynamics Simulation. The large-scale model of 55-component Jincheng anthracite ($C_{7730}H_{3916}O_{133}N_{123}S_{25}$) was selected [29]. The unit cell size of the anthracite model is $5.4 \times 4.8 \times 5.5\,nm^3$ ($x{\cdot}y{\cdot}z$), and the model density is $1.43\,g/cm^3$. A surfactant-anthracite binary system and a water-surfactant-anthracite ternary system were constructed. The surfactant layers containing 10 molecules and the water layer containing 2000 molecules were constructed. When the Tween 20 model was constructed, the average structure was adopted [31–33] that was $x = y = z = w = 5$. Molecular dynamics simulations were performed in Materials Studio 8.0. The COMPASS force field was used to describe the intermolecular interactions. Before the MD simulation, the energy of all models was minimized using the smart algorithm. NVT ensemble was used for MD simulation. Nose was used for thermostat [11]. The time step was set to

Table 1: Ultimate analyses of Jincheng anthracite.

C	H	O	N	S
91.51	3.89	2.10	1.71	0.79

1 fs. The temperature was 298 K. In all MD simulations, the Ewald algorithm was selected for long-range electrostatic interaction, the accuracy was 0.001 kcal/mol, the atom-based algorithm was selected for the van der Waals interaction, and the cutoff distance was 1.25 nm. A 12 nm vacuum layer was added to the surface of each model to eliminate the mirror effect. The bottom two-thirds of the anthracite model is fixed. In systems with larger atomic weights, this approach will save computation time considerably. According to Zhang et al. [25], this operation did not affect the calculation results.

Herein, Figure 2 shows that during the MD simulation, the interaction of water, surfactant, and anthracite were examined in two stages. The adsorption of the surfactant and anthracite was the initial stage, which allowed researchers to investigate the microscopic conformation and energy of the two's adsorption process. A surfactant coating was applied to the anthracite surface at this point, followed by a 1000 ps MD simulation using the NVT ensemble. The second stage was the interaction of water molecules with the surface of modified anthracite, which could be utilized to investigate changes in surfactant-modified anthracite's surface wettability. A 500 ps MD simulation was performed at this stage. As a comparison, MD simulations of water-anthracite were also performed.

2.3. Experiment

2.3.1. Surfactant Adsorption. Prior to the follow-up experiment, an adsorption test on the pickled coal sample was required to ensure that the surfactant was adsorbed on the anthracite surface and the concentration of different types of surfactant solution was 200 mg/L. When the concentration surfactant solution is 200 mg/L, it is higher than the critical micelle concentration (CMC). At room temperature, the CMC of $C_{12}(EO)_{20}$ is 90.1 mg/L [34, 35] and the CMC of Tween 20 is 67.5 mg/L [31, 36]. A 500 mg acid-washed coal sample was mixed with 500 mL of surfactant solution, and the solution was placed in a water bath with a magnetic stirring device and stirred at a constant speed (800 r/min) for 10 h at room temperature. The solution was centrifuged in a centrifuge (2000 r/min, 30 min), the obtained coal sample was vacuum filtered three times, and the residual surfactant solution in the coal was washed with DI water. The obtained solid wet anthracite samples were dried in a vacuum drying oven at 105°C for 2 h, cooled, sealed, and used for subsequent XPS tests.

2.3.2. XPS Measurements. XPS experiments were performed using a Thermo Scientific K-Alpha X-ray electron spectrometer, and a monochromatic Al target (Kα hν = 1486.6 eV) was used as the X-ray source. During the test, the vacuum degree of the analysis chamber was better than 5.0E − 7mBar. The full-spectrum scan pass energy was 100 eV, and the resolution of the measurement scan was 1 eV. The narrow-spectrum scan was performed for 5 cycles of signal accumulation (different scan times for different elements), the pass energy was 50 eV, and the step size was 0.05 eV, which was used for the scan of C 1s and O 1s. The binding energy was charge corrected for the spectrum by contaminating carbon (C 1s = 284.8 eVe). The background effects were subtracted using Shirley's method.

3. Results and Discussion

3.1. Simulation Results

3.1.1. Roughness. Both experimental and theoretical studies have shown that the surface of anthracite is covered with potholes. The roughness and the size of the surface area can reflect the morphology of the anthracite surface. The surface area was calculated using a probe with a radius of 0.14 nm, which is roughly equivalent to the size of a water molecule. The calculated surface area and corresponding roughness are listed in Table 2. The roughness is defined by Eq. (1):

$$C = \frac{S}{L}. \tag{1}$$

Where$C$ represents the roughness, S represents the surface area, and L represents the unit cell projected area.

The unit cell projected area is the projected area of the unit cell on the xy plane. A roughness value of 1 indicates a perfectly smooth surface at the atomic level, while a value greater than 1 indicates that the surface has some degree of wrinkling. As seen in Table 2, the surface roughness of anthracite is greater than 1, indicating that the surface is rough and uneven, which is consistent with the real surface of anthracite. The surface of the anthracite after the adsorption of the surfactant becomes more rough, which is beneficial to the contact between the surface of the anthracite and the water molecules. Moreover, the surface of the anthracite after adsorption of Tween 20 is rougher, which is presumed to be due to the more branched structures in the hydrophilic head group of Tween 20.

3.1.2. Interaction Energy. When two materials are adsorbed, the adsorption energy is used to calculate the interaction energy. The lower the adsorption energy, the more energy is released during the adsorption process between the two materials, resulting in a higher interaction energy between them [37–39]. The adsorption energy is defined by Eq. (2):

$$\begin{aligned} \mathrm{EV} &= \mathrm{EV}_{\mathrm{total}} - \mathrm{EV}_{\mathrm{A}} - \mathrm{EV}_{\mathrm{B}}, \\ \mathrm{EE} &= \mathrm{EE}_{\mathrm{total}} - \mathrm{EE}_{\mathrm{A}} - \mathrm{EE}_{\mathrm{B}}, \\ E &= \mathrm{EV} + \mathrm{EE}, \end{aligned} \tag{2}$$

Where EV stands for van der Waals interaction energy, EE stands for electrostatic interaction energy, E stands for total interaction energy, $\mathrm{EV}_{\mathrm{total}}$, $\mathrm{EE}_{\mathrm{total}}$ represents the total energy after the adsorption of the two materials is completed, EV_{A},

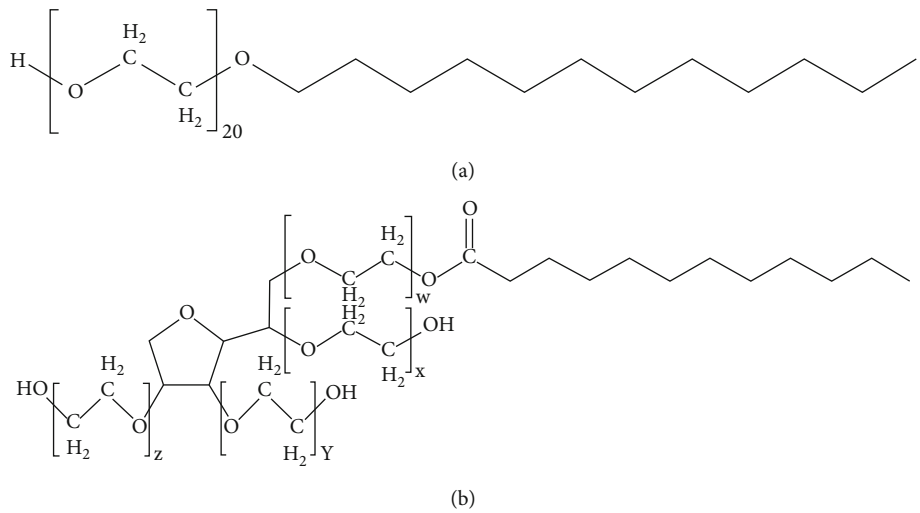

Figure 1: Chemical structure of surfactants, (a) $C_{12}(EO)_{20}$ and (b) Tween 20 ($x + y + z + w = 20$).

EE_A represents the energy of material A, and EV_B, EE_B represents the energy of material B.

Firstly, the interaction energy of the surfactant when adsorbed to the anthracite surface was calculated to compare the interaction energy. Here, A stands for surfactant and B for anthracite. The calculation results are shown in Table 3.

From the total interaction energy data in Table 3, $C_{12}(EO)_{20}$ releases more energy, the adsorption configuration is more stable, the network structure formed is denser. Tween 20 emits less energy, and the network structure formed is relatively loose. This is because the existence of the branched structure prevents the molecules from approaching and intertwining with each other [6].

Further analysis of the van der Waals interaction energy and electrostatic interaction energy shows that the van der Waals interaction energy dominates the adsorption process of the two surfactants on the surface of anthracite and the electrostatic interaction energy only accounts for a small part. Anthracite is a high-rank coal with a minor negative charge on its surface due to the lack of oxygen-containing functional groups [8]. In this sense, the anthracite and surfactant molecules have a small number of atoms with differing charges, a minor charge difference between them, and mild electrostatic interaction between the oppositely charged sections. As a result, electrostatic interactions make up a very modest percentage of the total interaction energy. It should be pointed out here that although nonionic surfactant molecules are electrically neutral, the atoms in them are still charged. The proportion of electrostatic interaction energy in Tween 20 is much smaller than that of $C_{12}(EO)_{20}$. It is speculated that this is due to the existence of the branched structure in Tween 20, which makes the polar hydrophilic head group farther away from the coal surface and the nonpolar hydrophobic tail chain is closer to the coal surface, resulting in a smaller electrostatic interaction energy. This is consistent with the conclusion of the relative concentration distribution analysis below.

The water-raw coal and water-modified coal adsorption energies were then calculated to analyze the changes in anthracite wettability, and raw coal here refers to the coal after acid treatment.

Comparing the total interaction energy in Table 4, the anthracite after adsorption by Tween 20 releases more energy when it is adsorbed with water molecules, indicating that the surface of the modified coal is more hydrophilic at this time and Tween 20 can effectively improve the hydrophilicity of the anthracite surface. This is because the existence of the branched structure in the hydrophilic head group of Tween 20 increases the surface roughness, thereby increasing the contact probability with water molecules. And the loose layered structure is also conducive to the penetration of water molecules, so that the modified coal surface forms more hydrogen bonds with water molecules, and the adsorption force is stronger, thereby releasing more energy. This is consistent with abovementioned the roughness analysis and the hydrogen bond number analysis results below.

Further analysis of the van der Waals interaction energy and electrostatic interaction energy shows that the proportion of electrostatic interaction energy on the modified coal surface is greater than that of the van der Waals interaction energy, which also indicates that the surface of anthracite after adsorbing surfactants becomes hydrophilic. The proportion of electrostatic interaction energy in the Tween 20 system is 68.1% greater than that in the $C_{12}(EO)_{20}$ system, which is 57.8%, indicating that the surface of the anthracite after Tween 20 adsorption is more hydrophilic. This suggests that branched surfactants have better wetting properties for potential applications compared to linear surfactants [40]. This is consistent with the abovementioned analysis conclusion.

3.1.3. Relative Concentration Distribution. The relative concentration distribution of each component in the ternary system along the *Z*-axis was calculated, which could quantitatively reflect the adsorption capacity and visualize the structure of the adsorption layer. The relative concentration distributions of different systems along the *z*-axis are shown in Figure 3.

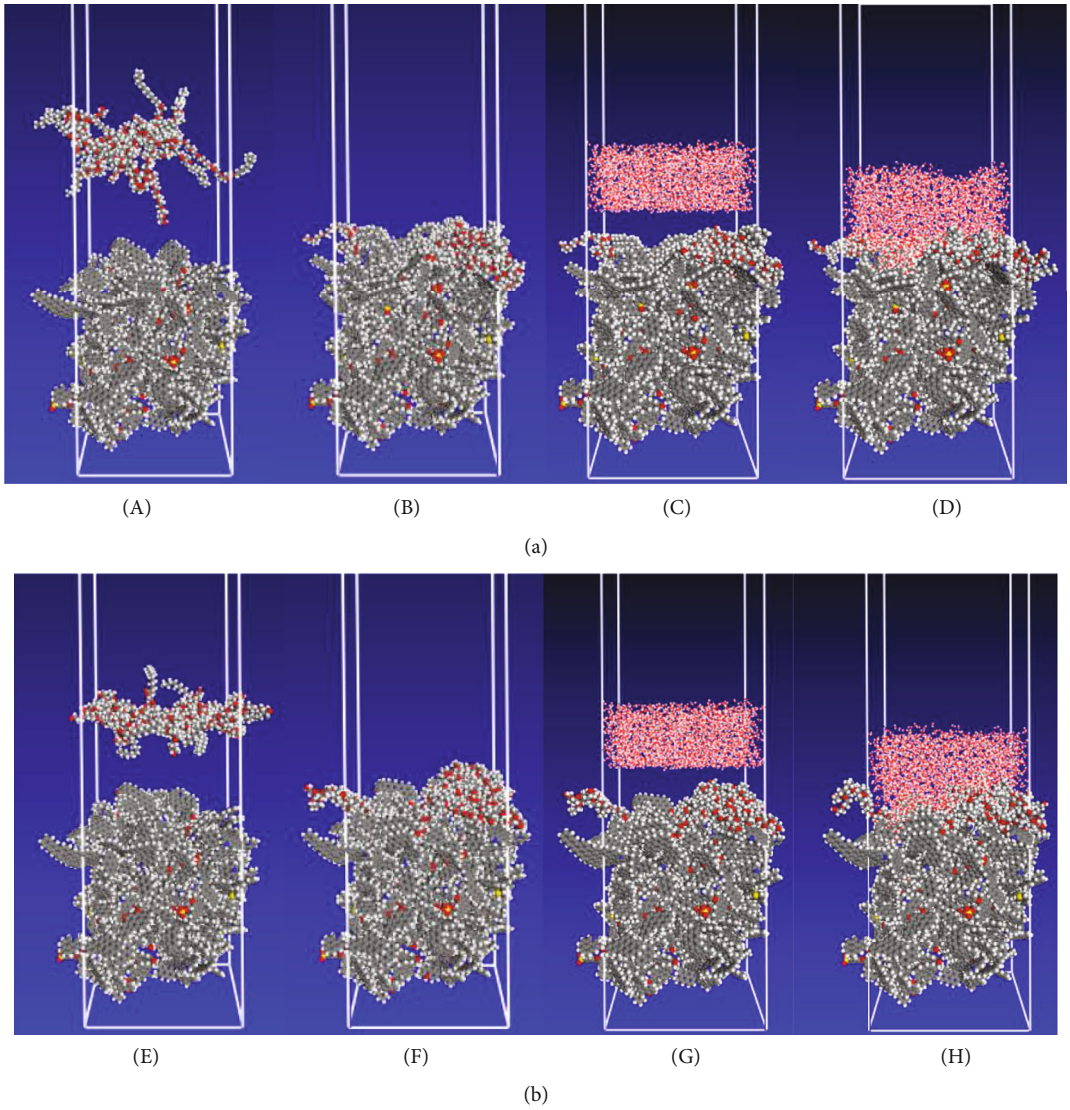

Figure 2: Adsorption process of surfactant on anthracite: (a) $C_{12}(EO)_{20}$ and (b) Tween 20. (A, E) Were the first-stage initial conformations, (B, F) were the first-stage final equilibrium conformations, (C, G) were the second-stage initial conformations, and (D, H) were the second-stage final equilibrium conformations.

Table 2: Surface area and roughness.

Model	S (nm^2)	L (nm^2)	Roughness
Anthracite	252.67	25.69	9.84
$C_{12}(EO)_{20}$-anthracite	304.37	25.69	11.85
Tween 20-anthracite	326.22	25.69	12.70

In the z-axis direction, the height of the coal model exceeds 7 nm, which is due to the choice of a multicomponent, high-molecular weight coal model. The starting point of the water layer in the Tween 20 system is 5.50 nm (the starting point is the abscissa value corresponding to when the relative concentration reaches 0.1), and the starting point of the water layer in the $C_{12}(EO)_{20}$ system is 6.14 nm. The permeability of water molecules in the Tween 20 system is stronger, because the network layer formed by it is relatively loose and the intermolecular gap is large, which is conducive to the penetration of water molecules. This is consistent with the abovementioned conclusion of the interaction energy analysis. Comparing the distribution of the hydrophobic tails in the two systems, the hydrophobic tails of Tween 20 shows a peak at 6.87 nm with a peak value of 20.30. The hydrophobic tail of $C_{12}(EO)_{20}$ takes a peak at 7.53 nm with a peak value of 18.93. This indicates that the hydrophobic tail chain of Tween 20 is closer to the surface of anthracite and the aggregation degree is higher. Comparing the distribution of hydrophilic head groups in the two systems, the peaks of Tween 20 and $C_{12}(EO)_{20}$ hydrophilic head groups are obtained at 7.23 nm and 7.12 nm, respectively, and the end points of the distribution of Tween 20 and $C_{12}(EO)_{20}$

Table 3: Adsorption energy between surfactant and anthracite.

Model	EV (kcal·mol^{-1})	EE (kcal·mol^{-1})	E (kcal·mol^{-1})
$C_{12}(EO)_{20}$-anthracite	−509.21 (87.7%)	−71.25 (12.3%)	−580.46
Tween 20-anthracite	−431.86 (96.5%)	−15.70 (3.5%)	−447.56

Table 4: Adsorption energy between water and raw or modified coal surface.

Model	EV (kcal·mol^{-1})	EE (kcal·mol^{-1})	E (kcal·mol^{-1})
Water-raw coal	−380.36 (67.8%)	−180.95 (32.2%)	−561.31
Water-$C_{12}(EO)_{20}$-coal	−227.96 (42.2%)	−312.37 (57.8%)	−540.33
Water-Tween 20-coal	−261.51 (31.9%)	−557.26 (68.1%)	−818.77

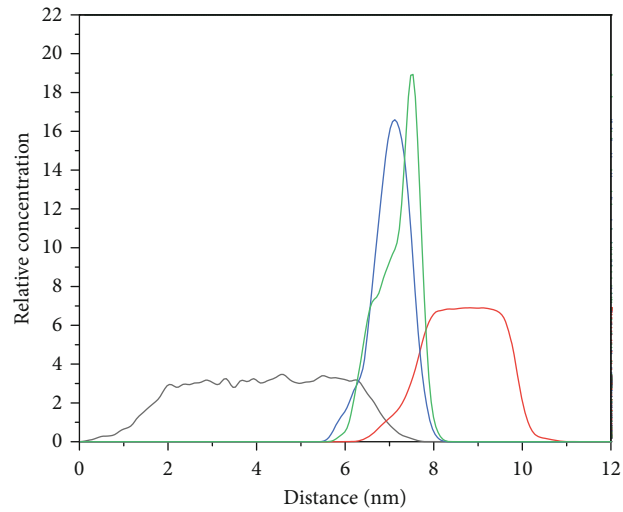

(a)

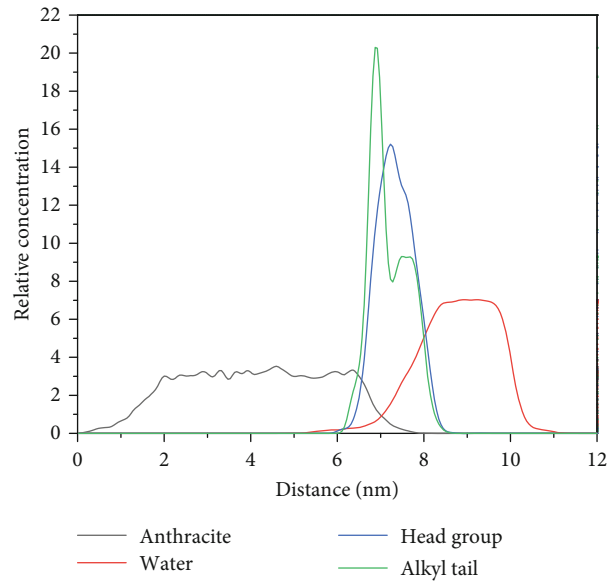

(b)

Figure 3: Relative concentration distribution along the z-axis: (a) water-$C_{12}(EO)_{20}$-anthracite system and (b) water-Tween 20-anthracite system.

hydrophilic head groups are 8.55 nm and 8.15 nm, respectively. It means that the hydrophilic head group of Tween 20 is closer to the water phase.

Comparing the distribution of the hydrophilic head group and hydrophobic tail chain in Tween 20, the hydrophobic tail chain peaks at 6.87 nm, the hydrophilic head group peaks at 7.23 nm, and the hydrophobic tail chain is closer to the coal surface. It shows that the adsorption structure is that the hydrophilic head group wraps the hydrophobic tail chain, that is, the hydrophobic tail chain faces the coal surface and the hydrophilic head group faces the water phase.

Comparing the distribution of the hydrophilic head group and hydrophobic tail chain in $C_{12}(EO)_{20}$, the hydrophobic tail chain peaks at 7.53 nm, the hydrophilic head group peaks at 7.12 nm, and the hydrophilic head group is closer to the coal surface. It shows that the adsorption structure is that the hydrophobic tail chain wraps the hydrophilic head group, that is, the hydrophobic tail chain faces the water phase and the hydrophilic head group faces the coal surface.

The abovementioned conclusion confirms the speculation in the abovementioned electrostatic interaction energy analysis.

3.1.4. Radial Distribution Function. The radial distribution function (RDF) between atoms can be used to calculate the coordination number and then determine the aggregation degree of B atoms surrounding A atoms. The radial distribution function between atoms forms a high and abrupt first peak, showing that the order is strong and the contact between atoms is strong [41–44]. RDF is determined using the Eq. (3):

$$g(r) = \frac{1}{4\pi\rho_B r^2} \cdot \frac{dN}{dr}. \quad (3)$$

Where$r$ represents the distance between B atoms and A atoms, ρ_B represents the density of B atoms, and dN is the average number of B atoms in the range from r to $r+dr$ (A is the reference atom).

First, the RDF between the oxygen atom in the surfactant ethoxy group (O_S) and the hydrogen atom in the water (H_W) was calculated. The RDF result is shown in Figure 4.

In both systems, the RDF curve peaks at around 0.18 nm and the peak value of the Tween 20 system is higher than that of $C_{12}(EO)_{20}$. It shows that the aggregation degree of water molecules on the coal surface after Tween 20 adsorption is higher; in other words, Tween 20 has a stronger binding ability to water molecules, making the modified anthracite surface more hydrophilic.

The coordination number was then multiplied by the aforesaid conclusion to arrive at a quantitative conclusion. The greater the contact between atoms, the higher the coordination number. The coordination number is determined using the Eq. (4).

$$dN = \frac{g(r) \cdot N \cdot 4\pi r^2 dr}{V}. \quad (4)$$

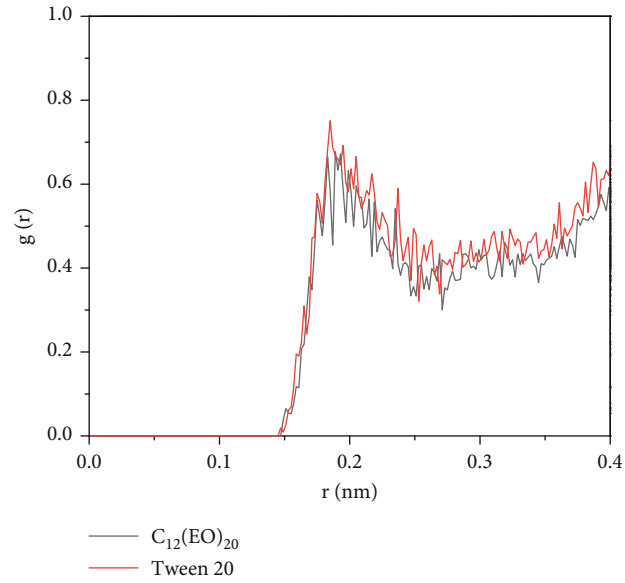

Figure 4: The RDF between O_S and H_W.

Table 5: The number of hydrogen bonds in different systems.

Model	Number of hydrogen bonds
Water-raw coal	17
Water-$C_{12}(EO)_{20}$-coal	57
Water-Tween 20-coal	88

Where N is the total number of B atoms and V is the periodic model volume.

The numbers of hydrogen atoms in the water molecule around the oxygen atom in the ethoxy group in Tween 20 and $C_{12}(EO)_{20}$ are 0.30 and 0.28, respectively. The aggregation degree of water molecules around Tween 20 is higher than that of $C_{12}(EO)_{20}$.

3.1.5. Number of Hydrogen Bonds. The difference in the number of hydrogen bonds between water and modified coal can be used to explain the difference in hydrophilicity. Geometric criteria were used to define the presence of hydrogen bonds: the intermolecular hydrogen acceptor distance was less than 0.25 nm, and the donor hydrogen acceptor angle was greater than 135° [45]. The calculation results are shown in Table 5.

The number of hydrogen bonds between the modified coal surface and water molecules is greatly increased after the addition of surfactants, indicating that such surfactants can improve the hydrophilicity of anthracite. There are more hydrogen bonds formed in the water-Tween 20-coal system, indicating that the modified coal is more hydrophilic at this time. This is consistent with the abovementioned interaction energy analysis results.

3.2. Validation of the Simulation Results. The carbon spectrum and the oxygen spectrum were fitted by peaks to investigate the presence of carbon and oxygen elements on the surface of modified coal, based on the difference in the

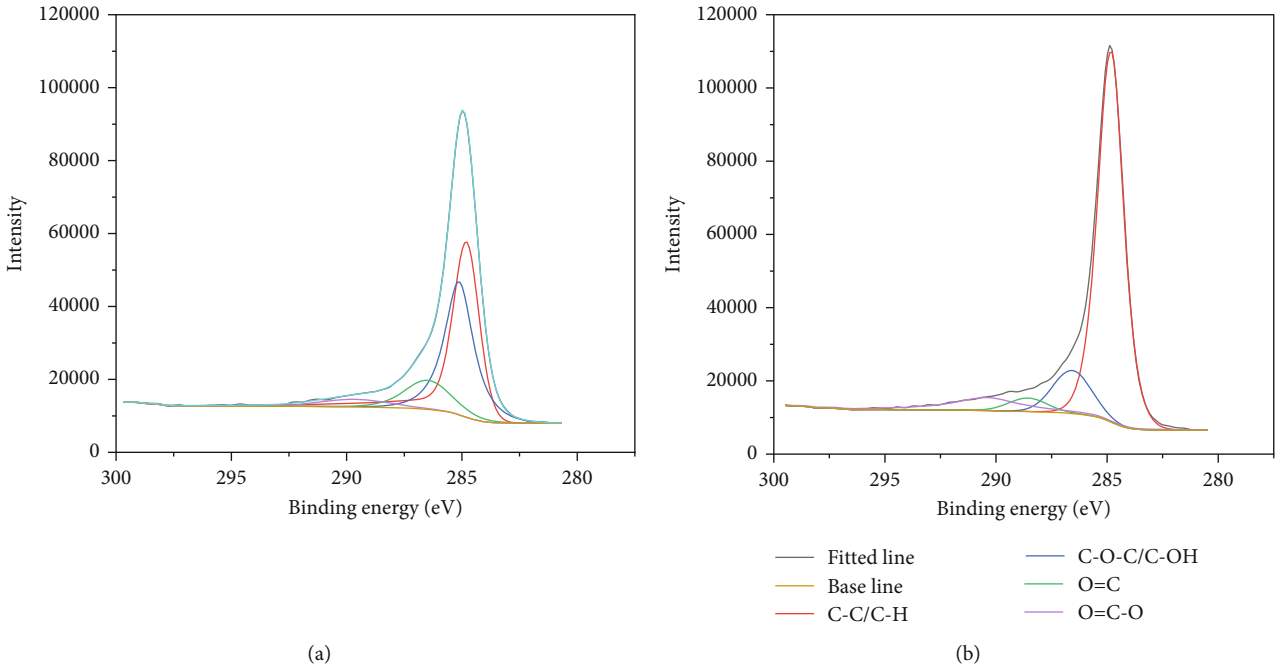

Figure 5: XPS spectrum of C 1s of anthracite after adsorbing different surfactants. (a) Tween 20-anthracite and (b) $C_{12}(EO)_{20}$-anthracite.

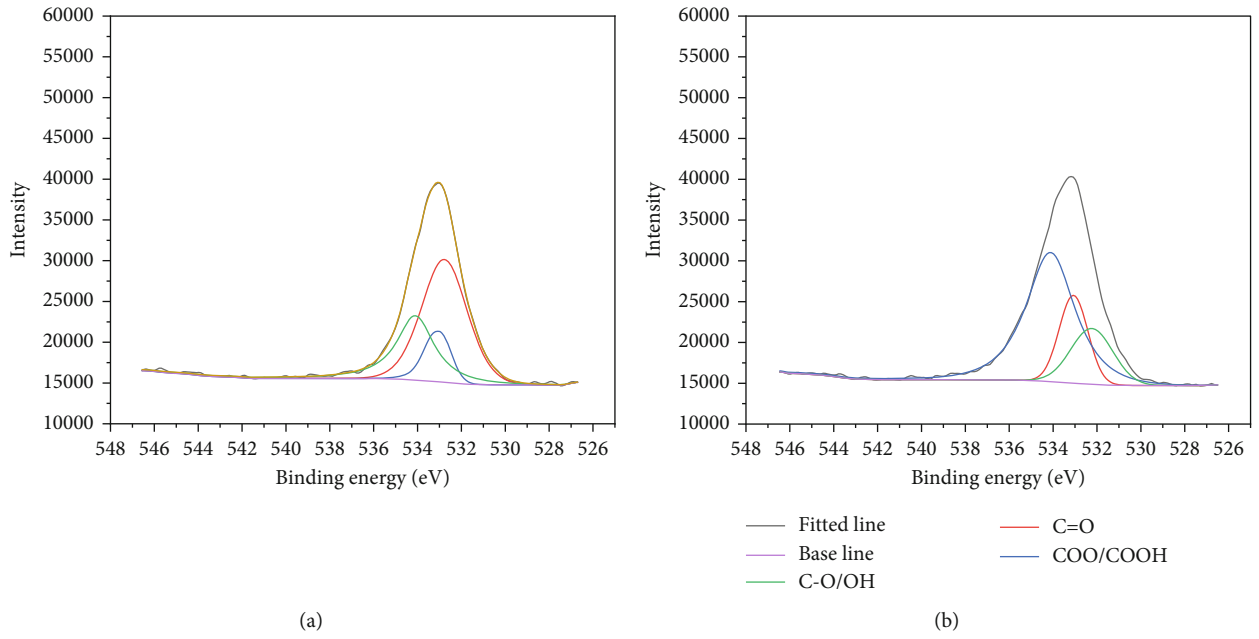

Figure 6: XPS spectrum of O 1s of anthracite after adsorbing different surfactants. (a) Tween 20-anthracite and (b) $C_{12}(EO)_{20}$-anthracite.

binding energy of electrons in the inner layer of atoms, and the XPS images of C 1s and O 1s on the surface of modified coal were obtained, and the results are shown in Figures 5 and 6, respectively.

3.2.1. C 1s Line Analysis. As seen in Table 6 that comparing the C-C/C-H content on the modified coal surface, the proportion after adsorption of Tween 20 is 45.0% and the proportion after adsorption of $C_{12}(EO)_{20}$ is 75.6%. Comparing the content of oxygen-containing functional groups, the proportion after adsorption of Tween 20 is 55.0% and the proportion after adsorption of $C_{12}(EO)_{20}$ is 24.4%. The surface carbon content of the coal modified by Tween 20 is lower, while the oxygen content is higher. This phenomenon indicates that the surface of coal modified by Tween 20 is more hydrophilic. This confirms the adsorption configuration obtained from the abovementioned relative concentration distribution, that is, the adsorption configuration of Tween

Table 6: Peak positions, areas, and atomic assignments of C 1s on the surface of anthracite after adsorption.

Groups	Tween 20		$C_{12}(EO)_{20}$	
	Binding energy (eV)	PR (%)	Binding energy (eV)	PR (%)
C-C/C-H	284.80	45.00	284.80	75.61
C-O	285.12	38.31	286.58	12.28
C=O	286.43	12.15	288.56	3.81
COO	289.62	4.54	290.43	8.30

Table 7: Peak positions, areas, and atomic assignments of O 1s on the surface of anthracite after adsorption.

Groups	Tween 20		$C_{12}(EO)_{20}$	
	Binding energy (eV)	PR (%)	Binding energy (eV)	PR (%)
C-O/OH	532.77	56.36	532.23	19.22
C=O	533.01	13.73	533.07	20.67
COO/COOH	534.09	29.91	534.12	60.10

20 is that the hydrophilic head group covers the hydrophobic tail chain, while the adsorption configuration of $C_{12}(EO)_{20}$ is that the hydrophobic tail chain covers the hydrophilic head group.

3.2.2. O 1s Line Analysis. As seen in Table 7, there are three kinds of oxygen atoms with different binding energies after adsorption of two different surfactants in anthracite coal. Among them, the contribution of C-O/OH functional groups on the coal structure is concentrated around the binding energy of 532 eV, the oxygen atom with binding energy around 533 eV is the contribution of C=O, and the binding energy around 534 eV is COO/COOH [46]. All oxygen-containing functional groups in $C_{12}(EO)_{20}$ are C-O/OH. Most of the oxygen-containing functional groups in Tween 20 are C-O/OH, with only a very small amount of C=O. The remaining oxygen-containing functional groups such as C=O and COO/COOH mainly exist on the surface of anthracite. Comparing the C-O/OH content on the modified coal surface, the C-O/OH ratio after modification by Tween 20 is 56.36% and the C-O/OH ratio after $C_{12}(EO)_{20}$ adsorption is 19.22%. In this case, the surface of the coal modified by Tween 20 is more covered by the hydrophilic head group of the surfactant, so it is more hydrophilic. Compared with the proportion of other oxygen-containing functional groups, the proportion of other oxygen-containing functional groups after modification by Tween 20 is 43.64% and that after modification by $C_{12}(EO)_{20}$ is 80.78%. This is due to the fact that the hydrophilic head group of $C_{12}(EO)_{20}$ is covered by its hydrophobic tail chain and thus cannot be exposed to the surface. Moreover, it preferentially adsorbs on the hydrophobic sites of anthracite during the adsorption process. The oxygen-containing functional groups on the surface of anthracite are exposed. The hydrophilic head group of Tween 20 covers its hydrophobic tail. This confirms the adsorption orientation derived from the relative concentration distribution.

4. Conclusions

In this investigation, molecular dynamics simulations and experiments were used to investigate the effects of two nonionic surfactants, lauryl polyoxyethylene ether $C_{12}(EO)_{20}$ and Tween 20, with different polyoxyethylene unit structures, on the wettability of anthracite.

Through molecular dynamics simulation, it is found that the surface of coal adsorbed by Tween 20 is more hydrophilic. The surface of anthracite becomes rougher after adsorption of two surfactants, and the surface roughness of anthracite after adsorption of Tween 20 is higher. The network layer formed by $C_{12}(EO)_{20}$ on the surface of anthracite is denser, while the network structure formed by Tween 20 is relatively loose. The branched polyoxyethylene structure is beneficial to the adsorption of surfactants and water molecules. The permeability of water molecules on the coal surface after Tween 20 modification is stronger, which confirms the conclusion that its network structure is looser. The adsorption configuration of Tween 20 is that the hydrophilic head group covers the hydrophobic tail chain, while the adsorption configuration of $C_{12}(EO)_{20}$ is that the hydrophobic tail chain covers the hydrophilic head group. The aggregation degree of water molecules near Tween 20 is higher, and more hydrogen bonds are formed between the surface of coal and water molecules after Tween 20 modification. The existence state of carbon and oxygen elements on the surface of modified coal was analyzed by XPS experiment, which confirmed the adsorption structure obtained by molecular simulation.

Molecular simulations are in good agreement with the experimental results. It shows that the branched polyoxyethylene unit can make the surface of anthracite more hydrophilic, which is more conducive to the suppression of anthracite dust. This study further explains the microscopic reasons why such surfactants can increase the hydrophilicity of anthracite. This research may provide useful guidance for rational design/selection of highly efficient coal dust suppressant.

Data Availability

The data used to support the findings of this study are included within the article.

Conflicts of Interest

The authors declare that there is no conflict of interest regarding the publication of this paper.

Authors' Contributions

Xuanlai Chen did the conceptualization, methodology, software, and writing—original draft preparation. Guochao Yan did the supervision, writing—reviewing, and editing. Guang Xu did the writing—reviewing and Editing. Xianglin Yang did the writing—reviewing and editing. Jiajun Li did the data curation, visualization, and investigation. Xuyang Bai did the data curation, visualization, and investigation.

Acknowledgments

This research was funded by the National Natural Science Foundation of China (Grant no. 51974195).

References

[1] Q. Zhou and B. Qin, "Coal dust suppression based on water mediums: a review of technologies and influencing factors," *Fuel*, vol. 302, article 121196, 2021.

[2] N. Guanhua, L. Zhao, S. Qian, L. Shang, and D. Kai, "Effects of [Bmim][Cl] ionic liquid with different concentrations on the functional groups and wettability of coal," *Advanced Powder Technology*, vol. 30, no. 3, pp. 610–624, 2019.

[3] G. Xu, Y. Chen, J. Eksteen, and J. Xu, "Surfactant-aided coal dust suppression: a review of evaluation methods and influencing factors," *Science of the Total Environment*, vol. 639, pp. 1060–1076, 2018.

[4] N. Guanhua, S. Qian, X. Meng et al., "Effect of NaCl-SDS compound solution on the wettability and functional groups of coal," *Fuel*, vol. 257, article 116077, 2019.

[5] S. K. Mishra and D. Panda, "Studies on the adsorption of Brij-35 and CTAB at the coal-water interface," *Journal of Colloid and Interface Science*, vol. 283, no. 2, pp. 294–299, 2005.

[6] X. Liu, S. Liu, Y. Cheng, and G. Xu, "Decrease in hydrophilicity and moisture readsorption of lignite: effects of surfactant structure," *Fuel*, vol. 273, article 117812, 2020.

[7] M. Yuan, W. Nie, W. Zhou et al., "Determining the effect of the non-ionic surfactant AEO9 on lignite adsorption and wetting via molecular dynamics (MD) simulation and experiment comparisons," *Fuel*, vol. 278, article 118339, 2020.

[8] S. Lyu, X. Chen, S. M. Shah, and X. Wu, "Experimental study of influence of natural surfactant soybean phospholipid on wettability of high-rank coal," *Fuel*, vol. 239, pp. 1–12, 2019.

[9] Q. Yao, C. Xu, Y. Zhang, G. Zhou, S. Zhang, and D. Wang, "Micromechanism of coal dust wettability and its effect on the selection and development of dust suppressants," *Process Safety and Environmental Protection*, vol. 111, pp. 726–732, 2017.

[10] B. Li, J. Guo, B. Albijanic, S. Liu, L. Zhang, and X. Sun, "Understanding flotation mechanism of nonionic surfactants with different polarity on kaolinite as a gangue mineral: an experimental and simulation study," *Minerals Engineering*, vol. 148, article 106226, 2020.

[11] R. Zhang, Y. Xing, Y. Xia et al., "New insight into surface wetting of coal with varying coalification degree: an experimental and molecular dynamics simulation study," *Applied Surface Science*, vol. 511, article 145610, 2020.

[12] J. Guo, L. Zhang, S. Liu, and B. Li, "Effects of hydrophilic groups of nonionic surfactants on the wettability of lignite surface: molecular dynamics simulation and experimental study," *Fuel*, vol. 231, pp. 449–457, 2018.

[13] Z. Liu, G. Zhou, S. Li, C. Wang, R. Liu, and W. Jiang, "Molecular dynamics simulation and experimental characterization of anionic surfactant: influence on wettability of low-rank coal," *Fuel*, vol. 279, article 118323, 2020.

[14] X. You, M. He, X. Zhu et al., "Influence of surfactant for improving dewatering of brown coal: a comparative experimental and MD simulation study," *Separation and Purification Technology*, vol. 210, pp. 473–478, 2019.

[15] X. You, M. He, W. Zhang et al., "Molecular dynamics simulations of nonylphenol ethoxylate on the Hatcher model of subbituminous coal surface," *Powder Technology*, vol. 332, pp. 323–330, 2018.

[16] Z. Chen, H. Qiu, Z. Hong, and G. Wang, "Molecular dynamics simulation of a lignite structure simplified model absorbing water," *Molecular Simulation*, vol. 46, no. 1, pp. 71–81, 2020.

[17] Y. Xia, Z. Yang, R. Zhang, Y. Xing, and X. Gui, "Enhancement of the surface hydrophobicity of low-rank coal by adsorbing DTAB: an experimental and molecular dynamics simulation study," *Fuel*, vol. 239, pp. 145–152, 2019.

[18] L. Zhang, B. Li, Y. Xia, and S. Liu, "Wettability modification of Wender lignite by adsorption of dodecyl poly ethoxylated surfactants with different degree of ethoxylation: a molecular dynamics simulation study," *Journal of Molecular Graphics & Modelling*, vol. 76, pp. 106–117, 2017.

[19] B. Li, J. Guo, S. Liu, B. Albijanic, L. Zhang, and X. Sun, "Molecular insight into the mechanism of benzene ring in nonionic surfactants on low-rank coal floatability," *Journal of Molecular Liquids*, vol. 302, article 112563, 2020.

[20] Y. Xia, Z. Yang, Y. Xing, and X. Gui, "Molecular simulation study on hydration of low-rank coal particles and formation of hydration film," *Physicochemical Problems of Mineral Processing*, vol. 55, no. 2, pp. 586–596, 2019.

[21] Y. Xia, R. Zhang, Y. Xing, and X. Gui, "Improving the adsorption of oily collector on the surface of low-rank coal during flotation using a cationic surfactant: an experimental and molecular dynamics simulation study," *Fuel*, vol. 235, pp. 687–695, 2019.

[22] B. Li, S. Liu, M. Fan, and L. Zhang, "The effect of ethylene oxide groups in dodecyl ethoxyl ethers on low rank coal flotation: an experimental study and simulation," *Powder Technology*, vol. 344, pp. 684–692, 2019.

[23] J. Guo, Y. Xia, Y. Liu, S. Liu, L. Zhang, and B. Li, "Microscopic adsorption behaviors of ionic surfactants on lignite surface and its effect on the wettability of lignite: a simulation and experimental study," *Journal of Molecular Liquids*, vol. 345, article 117851, 2022.

[24] X. Chen, G. Yan, X. Yang, and G. Xu, "Study on adsorption characteristics of sulfonate gemini surfactant on lignite surface," *Minerals*, vol. 11, no. 12, article 1401, 2021.

[25] Z. Zhang, C. Wang, and K. Yan, "Adsorption of collectors on model surface of Wiser bituminous coal: a molecular dynamics simulation study," *Minerals Engineering*, vol. 79, pp. 31–39, 2015.

[26] X. Chen, G. Yan, X. Yang, G. Xu, and S. Wei, "Microscopic diffusion characteristics of linear alkylbenzene sulfonates on the surface of anthracite: the influence of different attachment sites of benzene ring in the backbone," *Minerals*, vol. 11, no. 10, article 1045, 2021.

[27] X. Chen, G. Yan, G. Xu et al., "Computational study on the microscopic adsorption characteristics of linear alkylbenzene sulfonates with different chain lengths on anthracite surface," *Journal of Chemistry*, vol. 2022, Article ID 5318906, p. 17, 2022.

[28] S. Wei, G. C. Yan, Z. Q. Zhang, M. S. Liu, and Y. F. Zhang, "Molecular structure analysis of Jincheng anthracite coal," *Journal of China Coal Society*, vol. 43, no. 2, pp. 555–562, 2018.

[29] G. Yan, G. Ren, L. Bai, J. Feng, and Z. Zhang, "Molecular model construction and evaluation of Jincheng anthracite," *ACS Omega*, vol. 5, no. 19, pp. 10663–10670, 2020.

[30] X. Shang, K. Hou, J. Wu, Y. Zhang, J. Liu, and J. Qi, "The influence of mineral matter on moisture adsorption property of Shengli lignite," *Fuel*, vol. 182, pp. 749–753, 2016.

[31] Y. Liu, M. Liu, H. Yan et al., "Enhanced solubility of bisdemethoxycurcumin by interaction with Tween surfactants: spectroscopic and coarse-grained molecular dynamics simulation studies," *Journal of Molecular Liquids*, vol. 323, article 115073, 2021.

[32] M. Lapelosa, T. W. Patapoff, and I. E. Zarraga, "Molecular simulations of micellar aggregation of polysorbate 20 ester fractions and their interaction with N-phenyl-1-naphthylamine dye," *Biophysical Chemistry*, vol. 213, pp. 17–24, 2016.

[33] S. J. Marrink, H. J. Risselada, S. Yefimov, D. P. Tieleman, and A. H. De Vries, "The MARTINI force field: coarse grained model for biomolecular simulations," *The Journal of Physical Chemistry. B*, vol. 111, no. 27, pp. 7812–7824, 2007.

[34] X. Liu, S. Liu, M. Fan, J. Guo, and B. Li, "Decrease in hydrophilicity and moisture readsorption of Manglai lignite using lauryl polyoxyethylene ether: effects of the HLB and coverage on functional groups and pores," *Fuel Processing Technology*, vol. 174, pp. 33–40, 2018.

[35] Q. Jiaolong, P. Wenwen, Y. Xiaodong, Z. Teng, and R. Tianrui, "Studies on the surface properties of alcohol ethoxylate and the application in suspension concentrate," *Chemical Journal Of Chinese Universities-Chinese*, vol. 35, no. 10, pp. 2182–2190, 2014.

[36] R. Sanan and R. K. Mahajan, "Effect of fatty acid chain of tweens on the micellar behavior of dodecylbenzyldimethylammonium chloride," *Industrial and Engineering Chemistry Research*, vol. 50, no. 12, pp. 7319–7325, 2011.

[37] J. Li, Y. Han, G. Qu et al., "Molecular dynamics simulation of the aggregation behavior of N-dodecyl-N,N-dimethyl-3-ammonio-1-propanesulfonate/sodium dodecyl benzene sulfonate surfactant mixed system at oil/water interface," *Colloids and Surfaces A: Physicochemical and Engineering Aspects*, vol. 531, pp. 73–80, 2017.

[38] L. Li, M. He, Z. Li, C. Ma, H. Yu, and X. You, "Wettability effect of ethoxylated nonyl phenol with different ethylene oxide chain length on Shendong long-flame coal surface," *Materials Today Communications*, vol. 26, article 101697, 2021.

[39] M. H. Anvari, Q. Liu, Z. Xu, and P. Choi, "Molecular dynamics study of hydrophilic sphalerite (110) surface as modified by normal and branched butylthiols," *Langmuir*, vol. 34, no. 10, pp. 3363–3373, 2018.

[40] R. Ghosh, J. Dey, and B. P. Kumar, "Thermodynamically stable vesicle formation of biodegradable double mPEG-tailed amphiphiles with sulfonate head group," *RSC Advances*, vol. 10, no. 54, pp. 32522–32531, 2020.

[41] H. Yan, X. L. Guo, S. L. Yuan, and C. B. Liu, "Molecular dynamics study of the effect of calcium ions on the monolayer of SDC and SDSn surfactants at the vapor/liquid interface," *Langmuir*, vol. 27, no. 10, pp. 5762–5771, 2011.

[42] J. S. Yang, C. L. Yang, M. S. Wang, B. D. Chen, and X. G. Ma, "Crystallization of alkane melts induced by carbon nanotubes and graphene nanosheets: a molecular dynamics simulation study," *Physical Chemistry Chemical Physics*, vol. 13, no. 34, pp. 15476–15482, 2011.

[43] X. He, O. Guvench, A. D. MacKerell Jr., and M. L. Klein, "Atomistic simulation study of linear alkylbenzene sulfonates at the water/air interface," *The Journal of Physical Chemistry. B*, vol. 114, no. 30, pp. 9787–9794, 2010.

[44] T. Zhao, G. Xu, S. Yuan, Y. Chen, and H. Yan, "Molecular dynamics study of alkyl benzene sulfonate at air/water interface: effect of inorganic salts," *The Journal of Physical Chemistry. B*, vol. 114, no. 15, pp. 5025–5033, 2010.

[45] Y. Xu, Y. L. Liu, S. Gao, Z. W. Jiang, D. Su, and G. S. Liu, "Monolayer adsorption of dodecylamine surfactants at the mica/water interface," *Chemical Engineering Science*, vol. 114, pp. 58–69, 2014.

[46] C. Xu, D. Wang, H. Wang et al., "Experimental investigation of coal dust wetting ability of anionic surfactants with different structures," *Process Safety and Environmental Protection*, vol. 121, pp. 69–76, 2019.